**Sensing and identifying the improvised explosive device suicide bombers: people carrying wires on their body**


William P. Fox, John Vesecky and Kenneth Laws



*The Journal of Defense Modeling and Simulation: Applications, Methodology, Technology* published online 11 October 2010
DOI: 10.1177/1548512910384604

# Report Documentation Page

*Form Approved*
*OMB No. 0704-0188*



| 1. REPORT DATE | 2. REPORT TYPE | 3. DATES COVERED |
|---|---|---|
| **2010** | | **00-00-2010 to 00-00-2010** |

| 4. TITLE AND SUBTITLE | 5a. CONTRACT NUMBER |
|---|---|
| **Sensing and identifying the improvised explosive device suicide bombers: people carrying wires on their body** | 5b. GRANT NUMBER |
| | 5c. PROGRAM ELEMENT NUMBER |
| 6. AUTHOR(S) | 5d. PROJECT NUMBER |
| | 5e. TASK NUMBER |
| | 5f. WORK UNIT NUMBER |
| 7. PERFORMING ORGANIZATION NAME(S) AND ADDRESS(ES) **Naval Postgraduate School,Department of Defense Analysis,589 Dyer Road,Monterey,CA,93943** | 8. PERFORMING ORGANIZATION REPORT NUMBER |
| 9. SPONSORING/MONITORING AGENCY NAME(S) AND ADDRESS(ES) | 10. SPONSOR/MONITOR'S ACRONYM(S) |
| | 11. SPONSOR/MONITOR'S REPORT NUMBER(S) |

12. DISTRIBUTION/AVAILABILITY STATEMENT
**Approved for public release; distribution unlimited**

13. SUPPLEMENTARY NOTES

14. ABSTRACT

**We examined the use of radar to detect humans wearing detonation wires as part of a suicide vest in suicide bombings in an effort to stop the bombing. Dogaru et al. (Computer models of the human body signature for sensing through the wall radar applications. Tech. Rpt. ARL-TR-4290, Army Research Laboratory, 2007) used numerical electromagnetic simulations to show ways to use radar backscatter to detect humans carrying weapons behind walls. We developed Numerical Electromagnetic Code (NEC) simulations for the radar cross-section of wire configurations appropriate to the human body and compared them to the radar cross-section simulations for the human body done by Dogaru et al. We also used GunnPlexer Doppler radar at 12.5 GHz to collect laboratory experimental data from standoff distances of 2?8 meters from the following: human subjects, human subjects wearing a wire loop, and human subjects wearing a simulated vest with wire loops. We performed numerous experiments with both horizontal and vertical polarization (HH and VV), analyzing the data after each experimental run. We developed metrics from examining our experimental data of the radar cross-sections that could be used in building models to more accurately find subjects wearing wires. We wanted a metric to provide us with better statistical detection rates. We found several metrics that improved our ability to detect persons wearing wires. We discovered our best metric was the VV/HH ratio of radar cross-section. From our empirical modeling, we found that the ratio for people wearing wires was statistically different from people without wires at a level of significance of a = 0.05. Using this metric, we built a Monte Carlo simulation model that generated a crowd of people and randomly picked those with wires on their person. We used our metric and a threshold value which we determined experimentally, to distinguish the persons with wires from those without wires. We found from our simulation that our metric provided a success rate of detecting persons wearing wires of approximately 83.4%, based on running 36,000 trial runs in Excel. The rate of false alarms, where the metric in the simulation model picked a subject who was not wearing wires as a suspect wearing wires, was reduced to 28%. Using the work of Dogaru et al. and our NEC simulations of wire harnesses in the 0.85?1 GHz range, we found that the radar cross-section ratio (body with wires/body without wires) varied from 11 dB for 1?1.15 GHz VV polarization to ?5.5 dB for 0.85?1 GHz HH polarization. This frequency range was the best in the range 0.5?9 GHz. From our research we showed that we can be successful in finding viable metrics for detecting wires on people using radar observations. This preliminary research and the exciting results it produced encourages one to think that suicide bombers can be found prior to their detonation of their bombs and at ranges that are relatively safe.**

15. SUBJECT TERMS

| 16. SECURITY CLASSIFICATION OF: | | | 17. LIMITATION OF ABSTRACT | 18. NUMBER OF PAGES | 19a. NAME OF RESPONSIBLE PERSON |
|---|---|---|---|---|---|
| a. REPORT | b. ABSTRACT | c. THIS PAGE | | | |
| **unclassified** | **unclassified** | **unclassified** | **Same as Report (SAR)** | **21** | |

*Original article*

JDMS

Journal of Defense Modeling and Simulation: Applications, Methodology, Technology
XX(X) 1–20

DOI: 10.1177/1548512910384604
http://dms.sagepub.com

SAGE

# Sensing and identifying the improvised explosive device suicide bombers: people carrying wires on their body

**William P Fox[1], John Vesecky[2] and Kenneth Laws[2]**

**Abstract**

We examined the use of radar to detect humans wearing detonation wires as part of a suicide vest in suicide bombings in an effort to stop the bombing. Dogaru et al. (Computer models of the human body signature for sensing through the wall radar applications. Tech. Rpt. ARL-TR-4290, Army Research Laboratory, 2007) used numerical electromagnetic simulations to show ways to use radar backscatter to detect humans carrying weapons behind walls. We developed Numerical Electromagnetic Code (NEC) simulations for the radar cross-section of wire configurations appropriate to the human body and compared them to the radar cross-section simulations for the human body done by Dogaru et al. We also used GunnPlexer Doppler radar at 12.5 GHz to collect laboratory experimental data from standoff distances of 2–8 meters from the following: human subjects, human subjects wearing a wire loop, and human subjects wearing a simulated vest with wire loops. We performed numerous experiments with both horizontal and vertical polarization (HH and VV), analyzing the data after each experimental run. We developed metrics from examining our experimental data of the radar cross-sections that could be used in building models to more accurately find subjects wearing wires. We wanted a metric to provide us with better statistical detection rates. We found several metrics that improved our ability to detect persons wearing wires. We discovered our best metric was the VV/HH ratio of radar cross-section. From our empirical modeling, we found that the ratio for people wearing wires was statistically different from people without wires at a level of significance of $\alpha$ = 0.05. Using this metric, we built a Monte Carlo simulation model that generated a crowd of people and randomly picked those with wires on their person. We used our metric and a threshold value, which we determined experimentally, to distinguish the persons with wires from those without wires. We found from our simulation that our metric provided a success rate of detecting persons wearing wires of approximately 83.4%, based on running 36,000 trial runs in Excel. The rate of false alarms, where the metric in the simulation model picked a subject who was not wearing wires as a suspect wearing wires, was reduced to 28%.

Using the work of Dogaru et al. and our NEC simulations of wire harnesses in the 0.85–1 GHz range, we found that the radar cross-section ratio (body with wires/body without wires) varied from 11 dB for 1–1.15 GHz VV polarization to –5.5 dB for 0.85–1 GHz HH polarization. This frequency range was the best in the range 0.5–9 GHz.

From our research we showed that we can be successful in finding viable metrics for detecting wires on people using radar observations. This preliminary research and the exciting results it produced encourages one to think that suicide bombers can be found prior to their detonation of their bombs and at ranges that are relatively safe.

**Keywords**

central limit theorem, chi-squared goodness of fit, descriptive statistics, exponential distributions, radar cross-section, radar detection, suicide bombs, simulation models, target threshold

## 1. Background and Literature Review

In their annual report for FY08, the Joint IED Defeat Organization, JIEDDO,[1] presented data in figures showing their progress to defeat improvised explosive devices (IEDs). Their presentation did not distinguish between the various types of IEDs used.

[1]Department of Defense Analysis, Naval Postgraduate School, USA
[2]Department of Electrical Engineering, University of California Santa Cruz, USA

**Corresponding author:**
William P Fox, Department of Defense Analysis, 589 Dyer Road, Room 103F, Naval Postgraduate School, Monterey, CA 93943, USA.
Email: wpfox@nps.edu

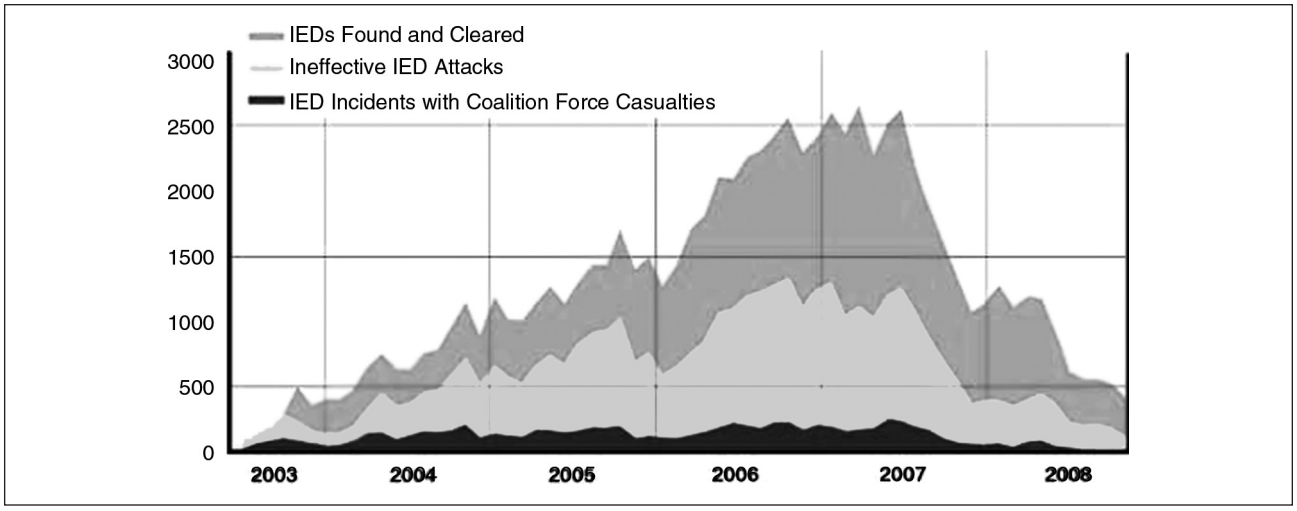


**Figure 1.** IED activity report by JIEDDO, 2003–2008.[1]

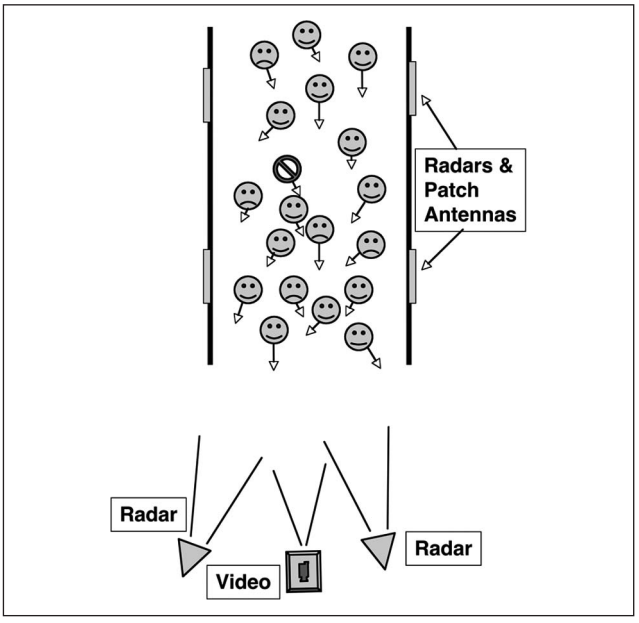


**Figure 2.** Radar observational geometry. One or more radars observe a group of people with one or two having wires on their bodies and hence becoming suspects.

We conclude from figure 1 that IEDs were and continue to be a major concern to the U.S. military, its allies, and the inhabitants of the region.

One major IED concern is the suicide bomber. The suicide bomber generally does not present their action prior to the event and can more easily accomplish their goal. We examine the dynamics involved in the suicide bomber and possible detection strategies using standoff radar.

The general observational situation we consider is illustrated in Figure 2. We see one or more radars observing a crowd of people of whom one or more have wires on their bodies and hence are suspects in terms of possible intent to do harm. We anticipate that the range from the radar to the people (or animals) under observation would be typically 50–100 meters. The concept is to make observations with one or more radars and likely other sensors as well, such as video surveillance cameras or thermal imaging. The results of these observations become the essential input data to our mathematical model that assesses the system's ability to detect *suspects* (persons suspected of harmful intent) from among a crowd of *subjects* who are largely harmless.

We discuss the radar observational systems, radar cross-sections of humans with and without wires on their bodies (from both experimental measurements and computational electromagnetic estimates), mathematical models with metrics, and our findings and conclusions with recommendations.

## *1.1 Radar Observational Metrics and System Design to Detect Wires on People*

Radar operates by generating radio waves, transmitting them through an antenna toward a target and then observing the radio waves that are scattered by targets and returned as echoes to the radar's receiving antenna. The movement of a person toward the radar causes a Doppler shift to the echo, making its frequency slightly higher and its wavelength slightly shorter, as illustrated in Figure 3.

The radar signal power echoed from a compact target is given by the radar range equation:

$$P_r(r) = (P_t G_t A_r RCS L_s)/(4 \pi r^2)^2 = (P_t G_t G_r \lambda^2 RCS L_s)/((4 \pi)^3 r^4) \quad (1)$$

where $P_r$ is power received in Watts, $P_t$ is power transmitted in Watts, $G_t$ is transmit antenna gain, $A_r$ is receiver

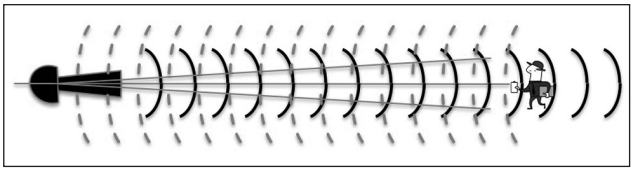

**Figure 3.** Basic principle of Doppler radar operation, shown for echoes from a moving person. Note that due to the Doppler effect of the person moving toward the radar, the radar echoes (dashed arcs) have a slightly shorter wavelength than the waves transmitted from the radar (solid arcs).

antenna area in $m^2$, *RCS* is radar cross-section in $m^2$, $L_s$ is the system loss factor, and $r$ is the range to target in m. We note that the right-hand version of the equation uses the relation that $G_r$ = receiver antenna gain = $4 \pi A_r/\lambda^2$, where $\lambda$ is the wavelength in meters.

Radars can measure a variety of characteristics of the target, principally range (via echo time delay), speed (via Doppler shift), and radar cross-section (via echo strength and characteristics). More details at a basic level can be found in excellent introductory books by Kingsley and Quegan[2] and Skolnik.[3] Due to the very close range of the target, tens of meters, determining range using pulses requires some care in radar design, since the round-trip travel time to the target and back is only 67 nanoseconds (for 10 m range). We used a pulse-Doppler radar in our preliminary work that can determine both speed and range.

The detection concept is to find moving targets (people or animals) with radar metrics related to wires being on the person, for example radar cross-section, polarization characteristics, or other measures. Our objective with this technique is not to identify suicide bombers definitively, but to provide a significant aid in separating out people who are more likely to have wires on their person and hence, represent threats.

## *1.2 Radar Measurements*

Radars are amazingly capable instruments that operate at day or night and in most weather conditions. Basic radar measurements produce: (a) location of a target in range and direction, measured in m and degrees; (b) target speed (along the radar ray path) in m/s; (c) radar cross-section (RCS) (characteristics of radar echoes that derive from target characteristics); and (d) fluctuations in the three measurements above. We discuss in more detail the background of prominent aspects of the radar cross-section measurements that we used in the model. Radar waves are typically polarized and the most common polarizations are VV (vertical polarization on transmit and vertical polarization on receive) and HH, where the transmitted and received polarizations are horizontal. Vertical polarization means that the radar wave has its electric field in the plane of incidence (typically perpendicular to Earth's surface for near-surface geometry). So VV implies that the transmitter launches V polarization waves and the receiver is most sensitive to V polarization waves in the radar echoes. H polarization waves have their electric fields perpendicular to V polarized waves and are typically parallel to Earth's surface. Similarly, HH implies that H polarized waves are transmitted and H polarization waves are received. The measurements above are interpreted in terms of our project objectives along the following lines. Range and direction measurements allow us to isolate suspects in terms of their location relative to the radar. In this preliminary study we do not make experimental measurements that include range. However, a more advanced (pulse-Doppler or frequency-modulated continuous wave (FMCW)) radar could make effective measurements of both range and target speed and is discussed below. By combining radar with either video observations or thermal imagining, the identification of a suspect can be narrowed to a small number of people, identified visually in a group. Target speed, determined by the Doppler shift of the radar echo, allows both metrics for identifying suspects, for example walking speed,[4] as well as tracking the suspect in a group using video images. The RCS characteristics of people allow identification of those who are carrying wires on their bodies using the radar metrics that we uncovered. Finally, fluctuations in speed (Doppler shift) and radar cross-section as a subject walks may provide further metrics for identifying suspects with wires.

Important obstacles in interpreting radar echoes from subjects are echoes from stationary objects in the field of the view of the radar, which are currently not of interest here. The echoes from these uninteresting objects are called clutter. A very important technique in removing clutter is called moving target discrimination or Doppler filtering. Radar echoes are shifted slightly in frequency by

$$\Delta f = V_r/(\lambda/2) \tag{2}$$

when they are returned from moving targets (with speed $V_r$ along the radar line of sight and radar wavelength ($\lambda$) in meters. Even a very simple radar can measure this frequency shift very precisely. We are fortunate that the subjects of our investigation are walking (Figure 2) and, thus, have an easily detectable Doppler shift to separate them from clutter, as shown in Figure 4. In Figure 4 we see three Doppler spectra collected in our laboratory experiments (with a $\lambda$ = 0.03 m wavelength radar) in which a person walks toward a Doppler radar. These spectra show a distinct peak at Doppler frequencies of about 70–90 Hz. Using Equation (1) we find that these peaks correspond to walking speeds of 1–1.3 m/s. As a measure of radar cross-section we use a metric, such as the height of the Doppler spectrum peak (associated with walking speed) or the area under the Doppler peak, thus avoiding stationary background clutter echoes with Doppler shifts near zero Hz.

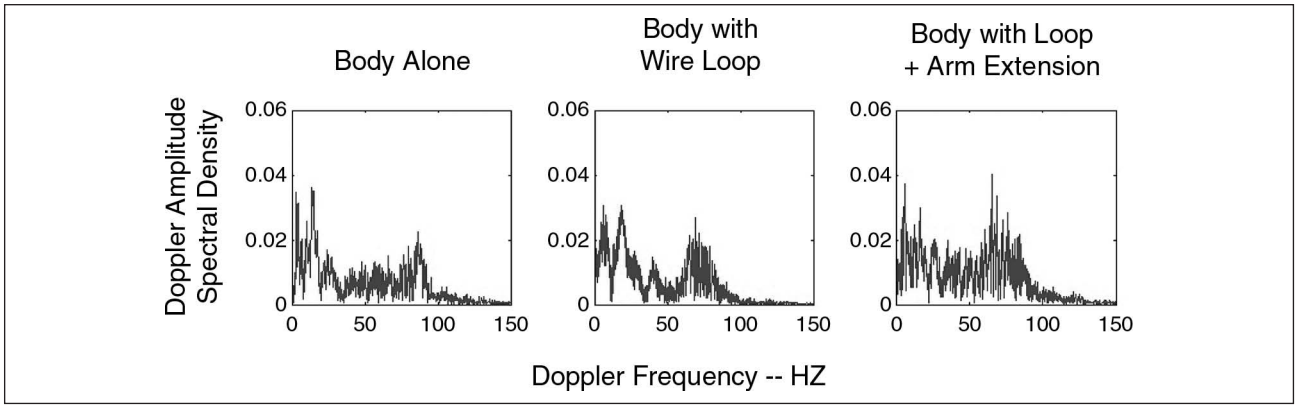


**Figure 4.** Doppler spectra of a person walking toward a 10.5 GHz CW radar in a laboratory experiment.

In their work, Angell and Rappaport[5,6] explained that while explosive devices have always been a formidable threat to civilians, as well as the military, the use of body-worn explosives poses a greater threat than ever before. Ever shrinking in size, these IEDs hide under the clothing of suicide bombers. The very nature of their improvised creation with non-standard parts makes it difficult to detect IEDs, particularly in a timely manner at a safe distance, to discriminate targets in azimuth at distances of up to 100 m. Radars can be made inexpensively and are safe and easy to use. In our modeling and analysis efforts we used a nominal standoff distance of 50 m.

The following explanation by Angell and Rappaport[5,6] is an assumption we made in our modeling efforts. One typical feature of body-worn IEDs is that they often tend to have outer metallic shells, resembling pipes or tubes. The metal casing not only increases the explosive's damage potential by projecting high-velocity shrapnel, but it also provides a detection characteristic. Circular metal cylinders have strong radar cross-sections, scattering incident radio frequency (RF) plane waves with characteristic patterns.

Although others have added additional clutter to the problem by using other objects, whether part of the explosives or part of normal non-uniformity in clothing, we have not. In other work, analysis has been done for the effects not only of objects added for increased damage with minimal effort, such as nails, but also the effects of varied clothing surfaces on the suicide bomber detection problem.[5,6]

According to work and analysis by Hamid,[7,8] Norgren,[9] Xu and Jo,[10] and Ciambra,[11] computational models have been used extensively for analyzing the scattered field patterns around cylindrical objects.

We considered, in turn, two methods of determining the radar cross-sections of bodies with and without wires attached: numerical electromagnetics and experimental measurements. A radar cross-section of the human body without wires has been modeled effectively by Dogaru et al.[12] using an anatomically correct model of the human body with the dielectric properties of the different body tissues, internal and external, specified on a computational grid.[13] They use the finite difference time domain (FTDT) technique, which is accurate and relatively simple in concept, but requires very significant computational resources.[14] The FTDT technique is based on Maxwell's time domain equations in discrete form. This leads to a set of FTDT update equations that allow estimation of the electromagnetic fields in a sample cell based on the values in neighboring cells obtained at the previous time step. Thus, starting with the initial values of the electromagnetic fields incident on the body at a given time, an electromagnetic wave can be propagated onto and into the body and the transmitted and scattered fields calculated in a time step (leapfrog) fashion. Dogaru et al.[12] checked their results in several different ways, comparing them with other simulation results. Further, our laboratory experiments agree rather well with their simulation (within 2 dB), particularly given the differences between our human subjects and the models discussed above. A cross-section of the torso of the fat man model is shown in Figure 5 and a cross-section of the body showing the different tissues that are used in the model is shown in Figure 6.

Dogaru et al.[12] investigated the RCS of the body at frequencies from about 500 MHz to 9 GHz in both VV and HH polarization. From our point of view the most important results from their work are shown in Figures 7 and 8, which indicate the possible analyses that are likely to be effective in separating suspects with wires on themselves from innocent subjects. Several important features emerge. The results of this detailed model indicate that at low frequencies, 0.5–1.5 GHz, where there is significant wave penetration into the body and absorption, the body has a relatively lower RCS when viewed from the front. At higher frequencies, where the radar echo is mainly from near the surface, the RCS is higher with notches of low RCS at intervals in frequency. This indicates that there are particular frequencies where the RCS is relatively low. However, aside from the region near 1 GHz, these notches are likely to change from body to body and vary with aspect angle, that is away from frontal view.

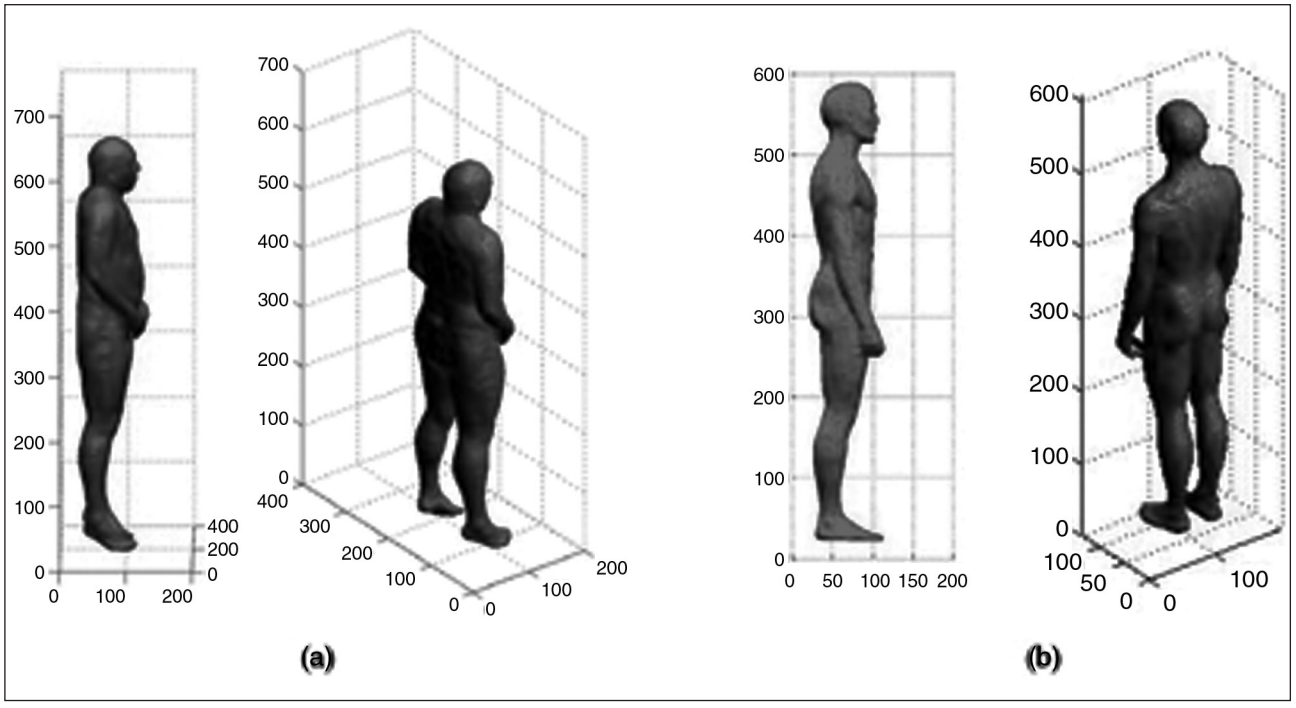


**Figure 5.** Rendering of fat man (a) and thin man (b) electrical models for the human body. The numbers are grid coordinates for the RCS modeling calculations. After Dogaru et al.[12]

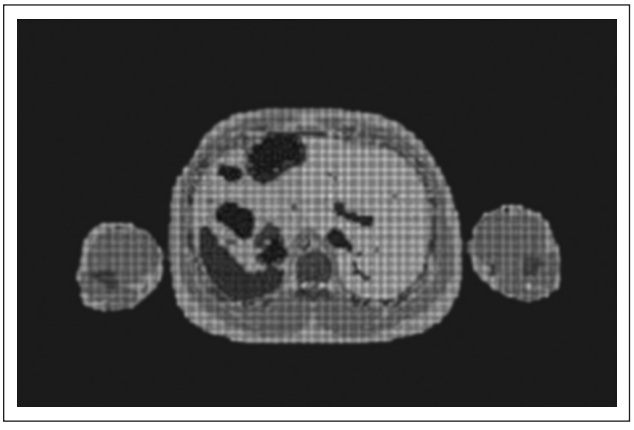

**Figure 6.** Cross-sectional view of the internal tissues of the torso of the fat man model. Each color represents a different kind of tissue, for example, skin, fat, muscle, and intestine. After Dogaru et al.[12]

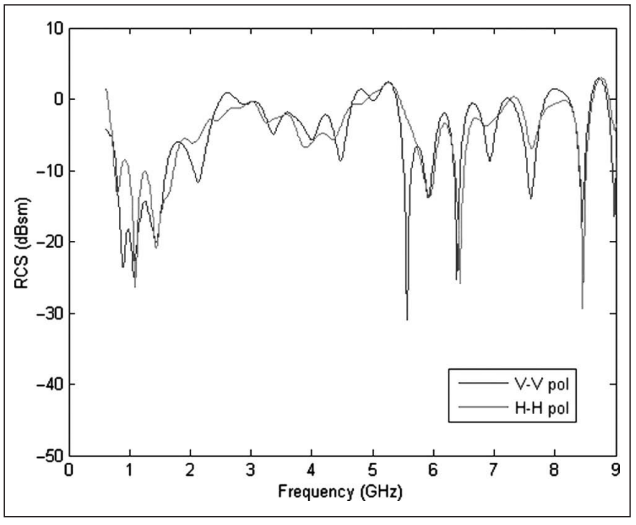


**Figure 7.** RCS of a simulated human body in both VV and HH polarization over the frequency range from 0.5 to 9 GHz. After Dogaru et al.[12]

So observations over a range of frequencies may well be needed to exploit signatures of wires on people. A second important feature, shown in Figure 7, is that the human body over much of the frequency range from 0.5 to 9 GHz exhibits VV and HH RCSs that are roughly equal.

This is because the human body does not have highly conducting linear features. In Figure 8 we see that a human body holding a highly conducting rod exhibits VV and HH RCSs that are significantly different over much of the frequency range examined. As we discuss below, this lead us to examine our own data for the same type differences. We discuss the metrics we came up with later.

To complement work by others (see above) we investigated radar backscatter properties of simulated vest wire configurations using the method of moments software, Numerical Electromagnetic Code (NEC).[15] The version of

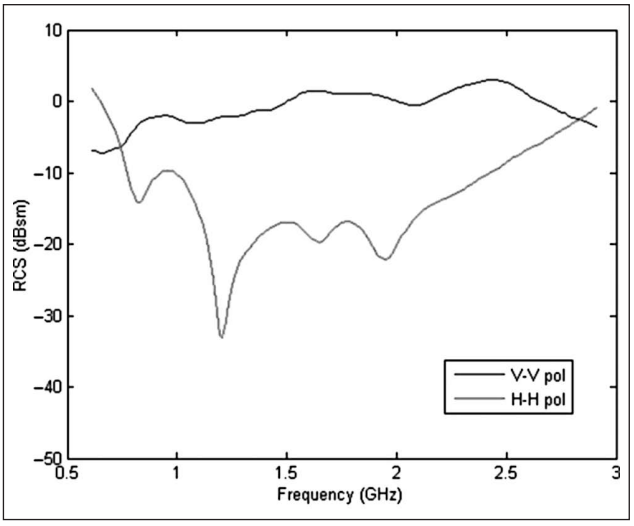


**Figure 8.** RCS of a human body carrying a thin, 1 m metal rod in front of the body. After Dogaru et al.[12]

NEC used here is NEC2, widely used and distributed free of charge (e.g. http://www.nec2.org/). A disadvantage to numerical electromagnetic calculations using the method of moments codes is that they are not well suited for analyzing the interaction between conductors and dielectrics. For this reason, the interaction between the human body and the vest configurations was not investigated here.

## 2. Problem Description

Over the course of the past 25 years, suicide attacks have emerged as one of the most effective methods used on a large scale by terrorist organizations. The willingness of an individual to sacrifice their own life in the course of an attack is a significant force multiplier when employed against a conventional security force. The purpose of suicide attacks is to create fear, mayhem, and chaos within a region. The doctrine of asymmetric warfare views suicide attacks as a result of an imbalance of power, in which groups with little significant power resort to suicide bombing as a convenient tactic to demoralize the targeted civilians or government leadership of their enemies. Suicide attacks or bombings have only been used in 10 of the 69 countries that have had violent uprisings in the last half century, but the effects of suicide attacks are much more lethal than most armed attacks.

Our problem focused on our ability to find metrics that can be synthesized from radar scanning that allows the user to detect possible suicide bombers. This technology can be employed in airports, market places, military check points, and other transportation centers, as well as anywhere a suicide bomber may present themselves. Our goal is to build a mathematical model to show that this technology is both possible and feasible as a first step in preventing these deadly suicide bombings. Our efforts would focus of three efforts. Firstly, we had to build an experimental lab to allow the radar to collect data on experimental subjects both carrying wires and not carrying wires. Secondly, we needed to analyze the data to ensure that our results were consistent with theoretical and previous research. We use our data to search for possible radar metrics to use in the mathematical model. Next, we would build mathematical models and a Monte Carlo simulation model to test the metrics to find if one metric provided more reliable results.

## 3. Methodology and Experimental Design

The estimations of the RCS were made by simulating an illuminating plane wave incident upon the simulated vest

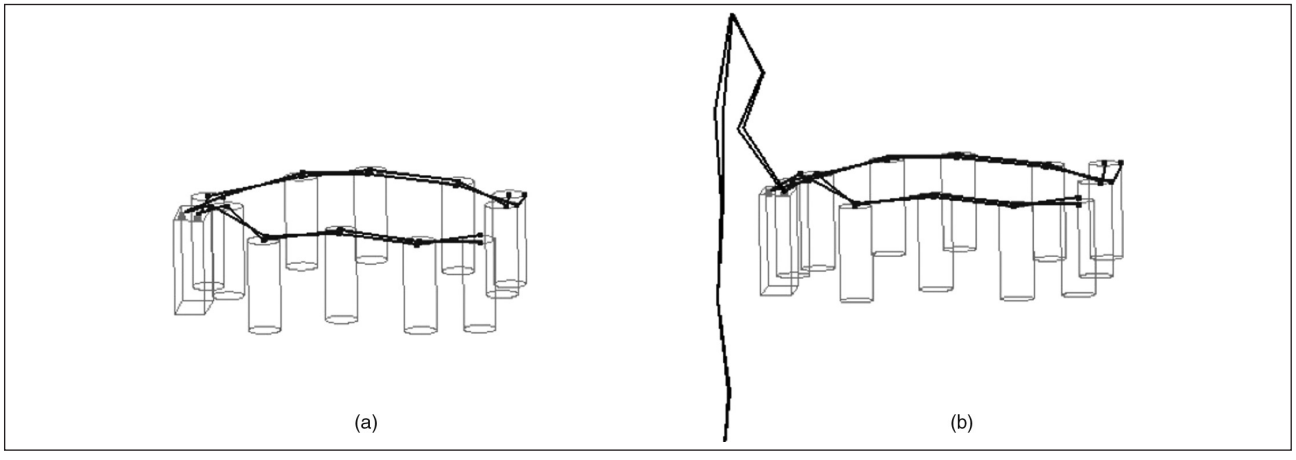


**Figure 9.** Two simple wire configurations for simulating explosive vests are shown. Vest 1 (a) contains only wires connected to igniters for explosives and a battery. Vest 2 (b) is a very similar wiring configuration, but includes also a pair of wires running under clothing, simulating the connection to a switch in the person's hand. The gray lines are to give an indication of locations of the battery and explosives and are to guide the eye only. They are not included in the simulation of radar backscatter. These viewing angles of the vests are defined relative to the *x* axis (horizontal in the plane of the page). Here the vests are viewed from between 270 and 360 degrees azimuth, polar angle less than 90 degrees.

wiring configurations. The simulated electric field was uniform with an intensity of 1 V/m. The simulated backscatter was computed for a field point at a distance of 50 m from the simulation grid origin. The RCS was then determined using

$$\sigma = 4\pi r^2 \frac{|E_s|^2}{|E_i|^2} \tag{3}$$

where $r$ is the distance between the scattering object and the observation point and $E_i$ and $E_s$ are the incident and scattered electric fields, respectively. The scattered field was calculated using NEC2 as a function of the azimuth angle $\phi_s$, the polar angle $\theta_s$, and the distance from the origin, $r$, (held constant at 50 m). Further details are given in Fox et al.[16]

Wire configurations investigated include those in Figure 9. The RCS for vest configurations was examined for two frequency ranges, firstly, centered on 10 GHz and secondly, centered on 1 GHz.

Data collection of the NEC calculations is shown in Figures 10(a) and (b), 11(a) and (b) and 12. In Figure 10 we show vest 1 from Figure 9 for both low and high microwave frequencies.

In Figure 10 we see that the HH polarization is consistently stronger as the wires in vest 1 are consistently more nearly horizontal (H) than vertical (V). Thus, the incident electric field of the radar signal is parallel to the wires for H polarization and excites stronger currents in the wires than does a radar signal with V polarization that has the electric field perpendicular to the wires. The peaks and valleys that occur as frequency changes are due to constructive and destructive interference between the radar

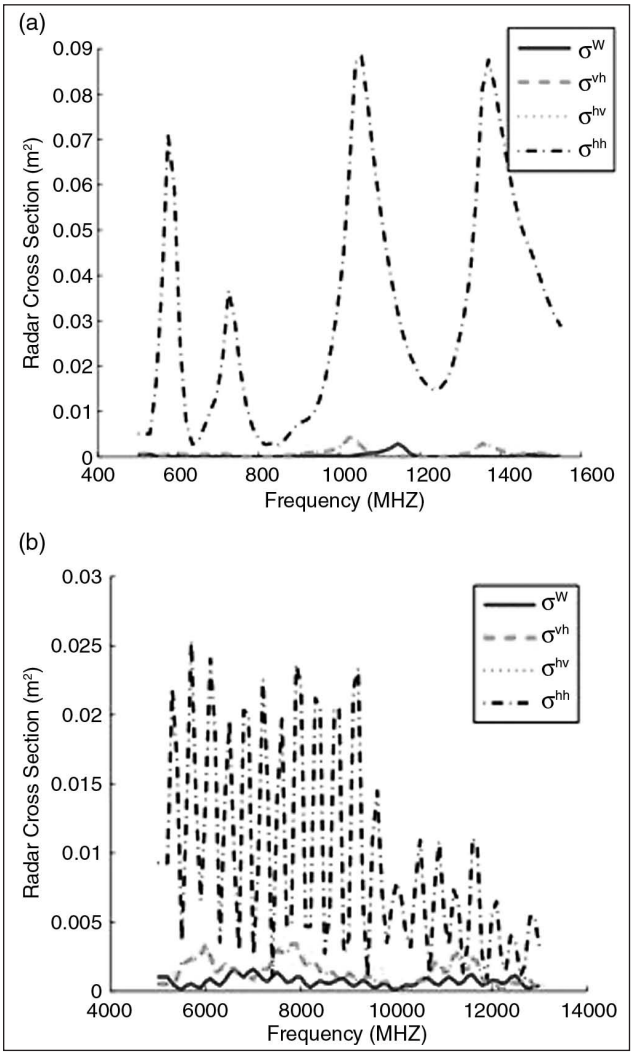


**Figure 10.** RCS of vest 1 from 0.5 to 1.6 GHz (a) and vest 1 from 5 to 13 GHz (b). The RCS is shown for all four permutations of transmit and receive polarization (VV, VH, HV, and HH). These RCS estimates were made using the NEC method of moments technique and or for a 0-degree azimuth (looking into Figure 9, perpendicular to the page).

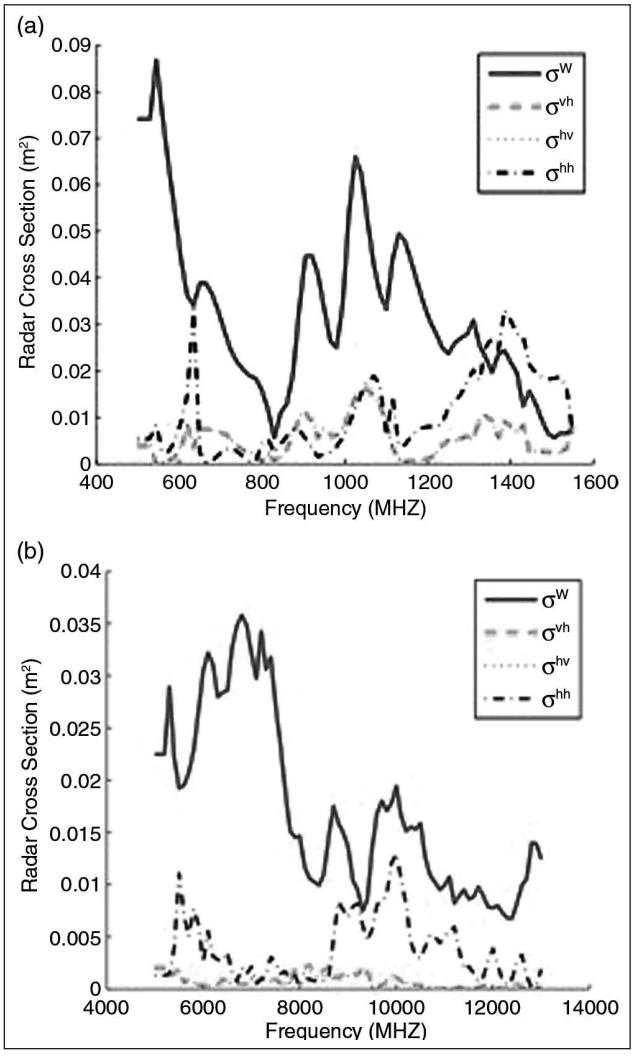


**Figure 11.** RCS of vest 2 from 0.5 to 1.6 GHz (a) and vest 2 from 5 to 13 GHz (b). The RCS is shown for all four permutations of transmit and receive polarization (VV, VH, HV, and HH). These RCS estimates were made using the NEC method of moments technique and are for a 0-degree azimuth (looking into Figure 9, perpendicular to the page).

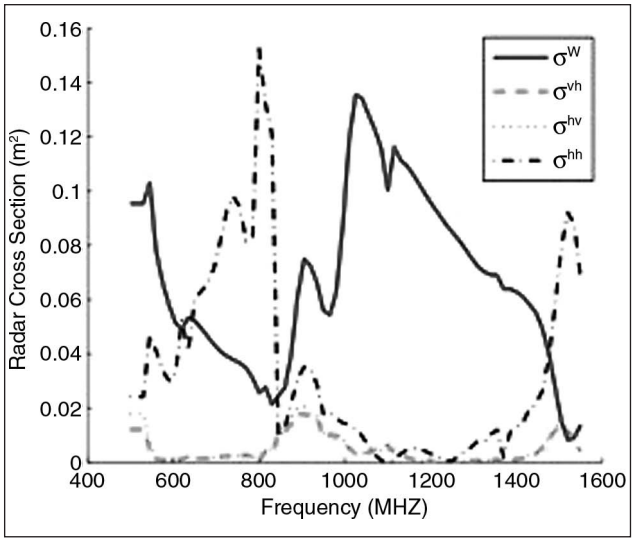


**Figure 12.** RCS of vest 2 from 0.5 to 1.6 GHz. The RCS is shown for all four permutations of transmit and receive polarization (VV, VH, HV, and HH). These RCS estimates were made using the NEC method of moments technique and are for a 90-degree azimuth (looking from the edge of Figure 9, parallel to the page).

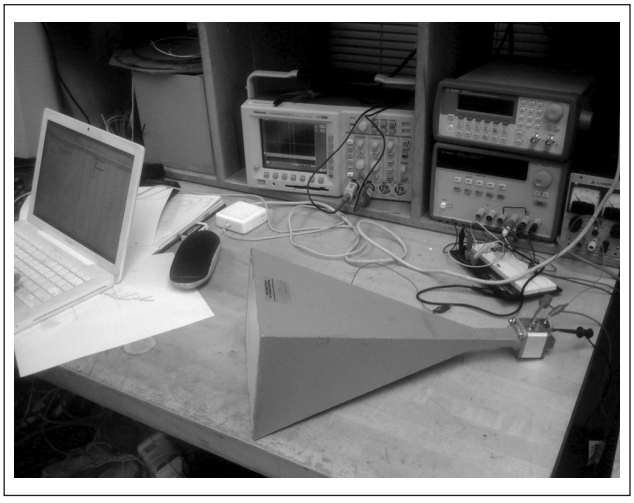

**Figure 13.** GunnPlexer experiment apparatus. The GunnPlexer CW Doppler radar is the small assembly at the small end of the horn antenna (blue–gray pyramid shaped structure).

echoes from different portions of the wire structure. This feature is common to nearly all complex conducting structures, such as airplanes.

In contrast to Figure 10 we see that in Figure 11 the VV polarization is consistently stronger, as the wires in vest 2 have some nearly horizontal (H) and some nearly vertical (V) elements. Thus, the incident electric field of the radar signal can excite strong currents in some of the wires regardless of whether the incident polarization is V or H. Again, the peaks and valleys that occur as frequency changes are due to constructive and destructive interference between the radar echoes from different portions of the wire structure. Since there are both horizontal and vertical structures in vest 2, VV and HH RCSs are more nearly equal in magnitude.

In Figure 12 we show the same vest as in Figure 11, but viewed at a 90° azimuth angle. For this case we see that either VV or HH polarization can dominate, depending on the frequency. This phenomenon is due to interference effects from the somewhat complex wire structure that contains both vertical and horizontal elements. Note that, regardless of the stronger polarization, one polarization or the other tends to dominate, that is they are seldom of equal strength.

We use a superposition approach in considering the suitability of RCS measurements as metrics for detecting people with wires present on their bodies in contrast to those without wires on their bodies. So we simply add the RCS of the body alone to the cross-section of the wires. Considering the results of Figures 7–12, we find several salient features. If we try to use only the RCS magnitude as a signature, we find that the RCS of the wires alone is typically smaller than the RCS of the human body alone, except for frequencies near 1 GHz. This indicates that aside from the frequencies near 1 GHz, we need to look elsewhere for a useful radar metric to separate *suspects* with wires on their bodies from innocent *subjects* without wires. Figures 7 and 8 tell us that the polarization ratio is a significantly better metric since, aside from a few frequencies, the polarization ratio for a body with wires is significantly different from 1 $m^2$ for the human body alone. This general conclusion is borne out in considering Figures 10–12. For nearly all frequencies either VV or HH cross-sections dominate – the VV and HH cross-sections are seldom nearly equal. Our experimental measurements confirm this conclusion. We examined the VV and HH differences.

In addition to numerical electromagnetic calculations, we performed a small number of experiments using a simple continuous wave (CW) Doppler radar already available in our laboratory. We took these experiments to confirm our numerical calculations and add observational data to our investigation to get a practical view of the problem. Although our analysis indicates that measurements in the 0.5–2.6 GHz range are most useful, we did not have a radar operating at all these frequencies available. Since the acquisition of radar instrumentation was beyond the scope of this research, we used apparatus on hand at the University of California at Santa Cruz, as shown in Figure 13.

In our experiments we used people with and without wires. The wires were used both with and without loops, corresponding to the two configurations shown previously in Figure 9. Three categories of experiments were conducted using the 10.525 GHz GunnPlexer Doppler Radar, shown in Figure 13. Since we wanted a high-quality signal, we restricted ourselves to the short ranges available in a small laboratory. These experiments are briefly described as follows.

(A) Pendulum experiments with vertical wires. In these experiments we were able to characterize the experimental apparatus and calibrate them in terms of a wire of known RCS.
(B) Body experiments with subjects walking toward the radar. In these experiments a person started from a marker ≈5 m from the radar and walked to a marker about 2 m from the radar. The person was observed without wires and with several different wire configurations on their bodies.
(C) Body experiments with subjects at approximately a constant range, swaying back and forth, toward and away from the radar, in order to generate a Doppler signal. These experiments gave a more consistent movement and were used in addition to those above to measure the RCS of a person with and without wires on their body.

We choose eight different cases for our experimental runs, collecting data for each case. The plots of these eight experiments are shown in Figure 14. The scatterplot of the data, along with the mean values, are plotted for a sequence of oscillating body experiments conducted along the lines of procedure C for:

no metal on person, VV polarization;
no metal on person, VV polarization, repeated;
no metal on person, HH polarization;
wire loop around waist, VV polarization;
wire loop around waist, HH polarization;
wire loop + wire under shirt sleeve going from waist to hand, VV polarization;
wire loop + wire under shirt sleeve going from waist to hand, VV polarization, repeated;
wire loop + wire under shirt sleeve going from waist to hand, HH polarization.

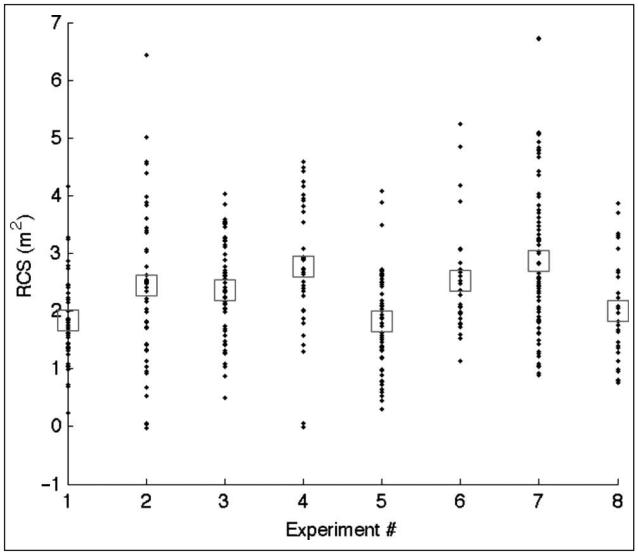


**Figure 14.** Measured RCS for the eight oscillating body subject experiments. Mean values are indicated by red squares (color online only).

A measure of uncertainty in the mean RCS estimate was obtained from the standard deviations of the values in each experimental column divided by the square root of the number of measurements. These data are summarized in Table 1. The advantage of these data relative to the earlier body RCS data (from numerical calculations), apart from an expected reduction in uncertainty, is the ability to estimate the experimental uncertainty from the multiple independent measurements obtained from each time series.

From previous reviewed work from the Army Research Laboratory (ARL)[12] we decided that looking at polarization might provide key insights. The polarization ratio was computed for these data as well and the results are summarized in Table 2. The polarization ratio was computed from the mean RCS for each experiment where matched VV and HH polarization data were available. The uncertainty in the polarization ratios is derived from the estimated uncertainty in the mean RCS values used. It is seen from the values in the table that differences in the polarization ratio between the experiments with metal on the person and no metal on the person are greater than the combined uncertainties.

**Table 1.** Mean RCS measurements of oscillating bodies.

| Number | Subject | Description | Pol. | RCS $m^2$ | $\delta_{RCS}$ $m^2$ |
|---|---|---|---|---|---|
| 1 | 1 | No metal | VV | 1.84 | 0.12 |
| 2 | 2 | No metal | VV | 2.44 | 0.19 |
| 3 | 2 | No metal | HH | 2.37 | 0.11 |
| 4 | 2 | Wire loop around waist | VV | 2.78 | 0.19 |
| 5 | 2 | Wire loop around waist | HH | 1.82 | 0.11 |
| 6 | 1 | Wire loop + wire in shirt sleeve | VV | 2.53 | 0.19 |
| 7 | 2 | Wire loop + wire in shirt sleeve | VV | 2.87 | 0.16 |
| 8 | 2 | Wire loop + wire in shirt sleeve | HH | 2.00 | 0.17 |

**Table 2.** Polarization ratio.

| Number | Description | RCS VV $m^2$ | RCS HH $m^2$ | Ratio | $\delta$ |
|---|---|---|---|---|---|
| 2 & 3 | No metal | 2.44 | 2.37 | 1.03 | 0.12 |
| 4 & 5 | Loop around waist | 2.78 | 1.80 | 1.52 | 0.15 |
| 7 & 8 | Loop + wire in sleeve | 2.87 | 2.00 | 1.43 | 0.11 |

Finally, we examined the data corresponding to subjects approaching the radar at a walking pace in terms of the spectral characteristics of the Doppler signals. We used three cases (no metal on person, wire loop around waist, and wire loop as well as wire from waist to hand going inside the shirt sleeve) in a variety of different scenarios. Example results were consistent with our Figure 4.

We must be able to detect and measure the properties of a target (human subject) with a RCS of 0.01 $m^2$ at a distance of 50 m with a signal-to-noise ratio (SNR) of about 15 dB, as well as obtaining Doppler shift (and spectra) information regarding the target. We summarize a candidate list of radar requirements as follows:

- detect a RCS = 0.01 $m^2$ target at 50 m with a SNR of 15 dB;
- use a radar frequency in the 0.5–15 GHz range to maximize the detection metrics;
- measure the Doppler spectrum of a person moving about 1 m/s to an accuracy of 0.1 m/s;
- locate a moving target to within a specified accuracy;
- radar design should be within easily achievable technology, that is not requiring heroic efforts, and be easily deployable from a small vehicle, for example a HumVee.

The starting point for a candidate radar design is the radar range in Equation (1). We want to find out what radar power is required to make a suitable measurement of a time series of echoes sufficient to measure the required Doppler shift, that is this is a pulse-Doppler radar. We rearrange the equation to solve for the required transmit power $P_t$ and include a factor ($n\,L_n$) that accounts for integration over a time series of pulses while a subject is within a range resolution cell and substitute $P_r = SNR \times (k\,T_o\,F\,Bw)$, where $(k\,T_o\,F\,Bw)$ is the noise in the $SNR$ and $P_r$ is the received signal power:

$$P_t(r) = [SNR\,(k\,T_o\,F\,Bw)\,(4\,\pi)^3\,r^4]/[n\,L_n\,G_t\,G_r\,\lambda^2\,RCS\,L_s] \quad (4)$$

where $k$ is Boltmann's constant, $T_o$ is the reference temperature (290 K), $F$ is the noise figure of the receiver, $Bw$ is the bandwidth of the radar, $n$ is the number of pulses that hit the target in the coherent integration time, that is while it is in a range resolution cell, $L_n$ is the loss in the coherent integration processing, $G_t$ and $G_r$ are the gains of the transmit and receive antennas and $RCS$ is the radar cross-section of the target.

The location of a target would be very helpful in isolating suspects with wires on their bodies. A radar can typically locate a target in a resolution cell, as shown in Figure 15, in range and azimuth coordinates. The radar bandwidth defines the range resolution cell by $\delta r = c/2Bw$, where $c$ is the speed of light. The azimuthal (angular) resolution cell is defined by $\delta\theta \approx \lambda/D$, where $D$ is the antenna width or diameter. It is easiest to see the impact of location considerations with

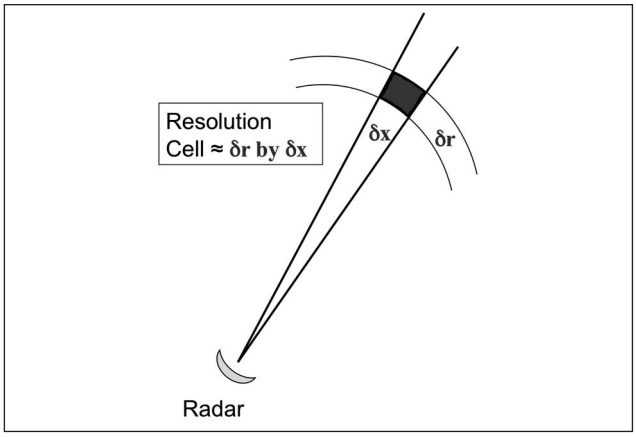


**Figure 15.** Azimuthal (angular) resolution cell

examples. Consider a range of 50 m, two radar frequencies 1 and 10 GHz and a half-meter antenna size. We take a typical radar bandwidth of 10% of the radar frequency.

The radar frequency is an important parameter as it is a focus of important system trade-offs. It is evident from Table 3 that the higher frequencies yield significantly better location resolution, particularly in lateral locations. At 10 GHz location resolution is excellent along the range direction and adequate along the azimuth direction. At 1 GHz location resolution is adequate along the range direction, but only marginally useful along the azimuth direction. Thus, from the point of view of location accuracy, the higher frequency is preferable. However, from the point of view of detection metrics, the lower frequency is likely to be better.

The antenna for the radar is likely to serve for both transmitting and receiving. Probably the best choice is a horn antenna that can cover a 2 to 1 or 3 to 1 range of frequencies. An example of a horn antenna for frequencies near 10 GHz is shown in Figure 13.

The speed measurement requirement of 0.1 m/s implies a Doppler frequency resolution requirement of 0.67 Hz (as per Equation (2)) for a 1 GHz radar and 6.7 Hz for a 10 GHz radar. This means that the 1 GHz radar must observe a target for an integration time of about 1.5 s and 0.15 s for a 10 GHz radar, so that the target should remain in a single resolution cell for at least these time periods. A walking person typically walks at no more than 2 m/s, so this requirement can be met with the values in Table 3.

**Table 3.** Target location capabilities of example radars.

| Radar frequency, $f$ in GHz | Range location resolution, $\delta r$ in m | Azimuth location resolution, $\delta x$ in m |
|---|---|---|
| 1 | 1.5 | 30 |
| 10 | 0.15 | 3 |

A fundamental limitation on the radar is that the pulse length cannot exceed the time needed to travel to the target and back. If we need to observe targets as close as 10 m, the maximum pulse length is about 67 ns or a minimum bandwidth of about 15 MHz. Knowing that radar bandwidth $Bw \approx c/(2\ \delta r)$ and consulting Table 3, we see that for bandwidths of about 100 MHz (1 GHz radar) and 1 GHz (10 GHz radar), 10% of the radar frequency, are quite adequate. So the minimum bandwidth is easily achieved by meeting the target location goals of Table 3. The very close proximity of targets, tens of meters, means that we must use short pulse lengths to prevent pulses from overlapping. Since pulse compression (chirp radar) is difficult technically for short pulses, it would be of limited advantage in this application.

We want to have a good SNR so we specify $SNR$ = 15 dB = a ratio of 32. Considering the background thermal noise, we get the required signal power from a radar pulse series, $P_r = SNR\ (k\ T_o\ F\ Bw)$. The noise ($k\ T_o\ F\ Bw$) is defined by Boltzmann's constant = 1.38 $10^{-23}$ J/K, $T_o$ = 290 K and the factors $F$ and $Bw$. The bandwidth $Bw$ is defined by Table 3 above and the noise figure, $F$, achievable at 1 and 10 GHz is ≈2 or less using MESFET or HEMPFET devices.

The pulse repetition frequency (PRF) is limited by a desire to have lots of pulses on the target to achieve a higher SNR and not wanting pulses to overlap. We choose $PRF$ = 3000 Hz, as this value is easy to achieve technologically and does not allow overlap for targets out to 50 km. Since 50 km is over the horizon and echoes from targets further away would be very weak, 3000 Hz seems a reasonable choice – it could probably be significantly higher. In 1.5 s this means that the number of pulses on a target within a coherent integration time is $n$ = 4500. We anticipate that the coherent integration will not be 100% efficient and so set $L_n$ = 0.8 (a typical number). Setting system losses $L_s$ = 0.5 is a typical rule of thumb.

We have now specified all the parameters in Equation (4) and can estimate the peak transmit power required for $r$ = 50 m, as shown in Table 4.

A solid-state transmitter at 1–10 GHz easily achieves these peak and average power levels. We note that the average power $P_{avg} = P_t\ PRF\ \tau \approx (P_t\ PRF)/Bw$, where τ is the pulse length, is very small. Thus, transmitter power consumption will not be a power consumption concern overall.

Conservative estimates of total power, weight, and volume should be of the order of tens of Watts, ≈10–20 lb (the antenna is a major factor and an antenna support has been excluded) and about a 1.5 ft cube or smaller, depending on the antenna. Our vision for an operational system would be the antenna and some electronics on an elevated mast 10 ft or more above ground level to prevent having to 'look' thorough a group of people. The bulk of the electronics (a cigar-box size, aside from prime power that we assume would come from a vehicle or mains supply) would be near the ground, connected to the antenna assembly by a cable and linked by wireless with a handheld display device for a soldier or policeman. While it is conceivable that a CW Doppler (GunnPlexer) type radar could be used in the fashion of a radar speed gun; the pulse-Doppler radar discussed above would provide more robust operation in terms of higher probability of detection and lower false-alarm rate. A thorough system design and prototype testing is needed to prove the effectiveness of our concept and sort out the relative advantages of candidate systems.

## 4. Results and Analysis

From the numerical modeling and experiments above we found several basic metrics as potential modeling metrics for the detection of *suspects* (people with wires on their bodies) in a group of *subjects* (innocent people without wires). These two metrics are the magnitude of the RCS (either VV or HH) and the 'polarization ratio' that is the ratio between these RCSs, for example ($RCS_{VV}/RCS_{HH}$). We further analyzed these to the difference and the ratio of the two polarizations. We found these to be most informative.

As seen previously from Figure 7, the RCS of the Human body (both VV and HH) is typically from 0.1 to a few $m^2$, except for the region around 1 GHz where it is as low as 0.01–0.1 $m^2$. Considering Figures 8 and 10–12, we find that the RCS (both VV and HH) of typical wire configurations is in the range 0.01–0.1 $m^2$. We conclude that straightforward use of the RCS magnitude as a metric is not feasible, except possibly in the frequency range near 1 GHz. More sophisticated methods with radar observations at multiple frequencies and polarizations may hold some promise, but are beyond the scope of this investigation.

As discussed in connection with Table 2, the use of the polarization ratio as a metric does hold promise. This can be illustrated by combining data from Figures 7 and 8. Figure 7 can be used to construct polarization ratio estimates for the human body alone and Figure 8 can be used to construct polarization ratio estimates for the human body

**Table 4.** Peak transmit power.

| Frequency, GHz | Bandwidth, GHz | Coherent integration time, s | Peak transmit power required, W | Average transmit power required, W |
|---|---|---|---|---|
| 1 | 0.1 | 1.5 | 0.005 | $1.5 \times 10^{-8}$ |
| 10 | 1 | 0.15 | 50 | $1.5 \times 10^{-3}$ |

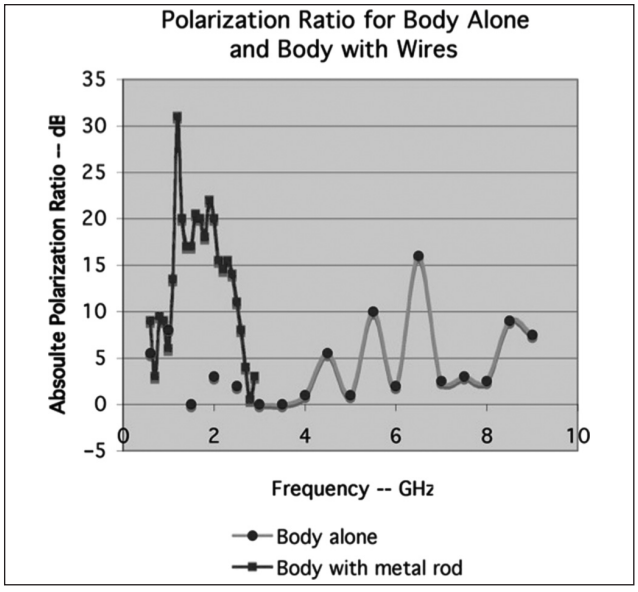


**Figure 16.** Comparison of polarization ratio (RCSVV/RCSHH) for the human body alone and the human body holding a metal rod. The data were taken from Dogaru et al.,[12] as shown in Figures 7 and 8.

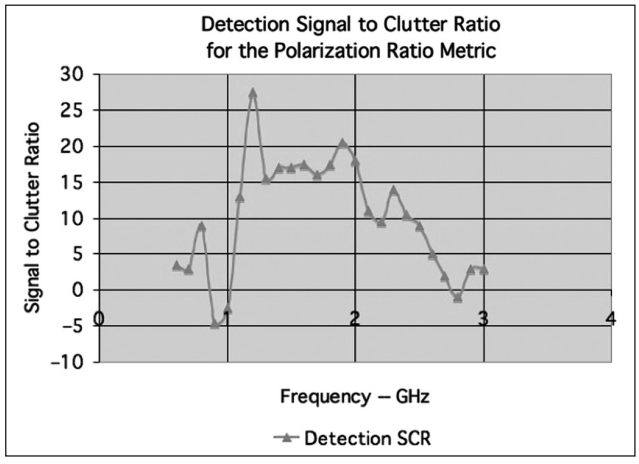


**Figure 17.** SCR calculated from the polarization ratio data of Figure 15.

holding a metal conductor. These estimates are combined in Figure 16. The comparison is limited to the frequency range of the data in Figure 8. In Figure 17 we have plotted the signal-to-clutter ratio (SCR), that is the ratio between the polarization ratio for the human body holding a metal rod and the polarization ratio for the human body alone.

We see from Figures 16 and 17 that the polarization ratio is a viable metric for detecting people with metallic conductors in a group of people without metallic conductors. Although the data of Figures 16 and 17 apply only to the frequency range near 1–3 GHz, the data in Table 2 cover the frequency range near 10 GHz. Thus, we conclude that the polarization ratio is a viable metric for our objectives. We summarize these results regarding radar metrics in Table 5.

As part of our analysis, we used the results of the experiments and began building and testing mathematical models. We started with radar detection probability. In radar detection theory, we are concerned with things such as how likely are we to detect the target and how often we make mistakes in detection. To answer these questions, we need probability theory.

In 1960, P Swerling developed the following exponential distributions. Equation (5) is used to describe different types of radar cross-sectional area fluctuations[2] that can be used dependent upon the analysis of scatters:

$$p(\lambda) = \frac{1}{\lambda_{\text{aug}}} e^{\frac{-\lambda}{\lambda_{\text{aug}}}}, \lambda \geq 0$$
$$p(\lambda) = \frac{4\lambda}{\lambda^2_{\text{aug}}} e^{\frac{-2\lambda}{\lambda_{\text{aug}}}}, \lambda \geq 0 \quad (5)$$

Of course we are concerned with both detection and false-alarm probabilities. We decided to use a threshold decision value, $Y$, such that the following events occur:[2]

target present: $y(t) > Y \rightarrow$ correct detection;
target present: $y(t) < Y \rightarrow$ missed detection;
target not present: $y(t) > Y \rightarrow$ false alarm;
target not present: $y(t) < Y \rightarrow$ no action.

In order to use Swirling's distribution, we tested our collected empirical data to ensure it followed an exponential distribution. We used a chi-squared goodness-of-fit test with our data to see if we could find the distribution that governs the behavior. We also looked for distinguishing patterns that may emerge that could lend themselves to discrimination for detection.

We examined both theoretical avenues presented, as well as empirical model building and analysis. In order to

**Table 5.** Radar metrics summary.

| Metric | Near 1 GHz | Near 10 GHz | Comments |
|---|---|---|---|
| RCS magnitude | Up to 10 dB in 200 MHz bands, variable | Not useful | Body RCS too high at 10 GHz |
| Polarization ratio | Robust, ≈1–2.5 GHz | Useful, but variable | Best across the board |
| Doppler features | Not evaluated | Walking speed & fluctuations | Relatively unexplored |
| Comments | Good metrics, but poor location capability | Polarization metric, good location | All metrics need further experiments |

build an appropriate model to detect a suicide bomber wearing a wire for detonation in a crowd, we must consider many simplifying assumptions.

### *4.1 Assumptions for the Model*

In any modeling effort, assumptions need to be made, since we cannot expect to capture all the factors influencing the identified problem.[16] The task is simplified by reducing the number of factors under consideration. Then, relationships among the variables may be determined. Again, by assuming relatively simple relationships, we can reduce the complexity of the problem.

- We assume, initially, a standoff range of 50 m from the radar to the targets.
- Modeling the use of one radar will give us valuable insights into the process of detecting suicide bombers.
- The suicide vests, explosives, and metal wires will be as we described earlier.
- Previous research in other radar detection studies provides valuable clues to the process, such as the radar cross-sectional area.
- Frequency will be critical, but we will restrict our analysis to the frequency band of our GunnPlexer radar on hand.
- Data can easily be collected on frequency, time, RCS, vertical and horizontal polarization, and with and without wires. Therefore, these will be the variables used in the modeling effort.
- We assume the speed (ft/sec) of the suicide bomber will be different (faster or slower) than the normal crowd.[4]
- Persons wearing wires will be suicide bombers. We assume no metal jewelry is worn nor will someone wear their cell phone around their neck. This is a simplifying assumption for this phase of the modeling and should be revisited in future modeling efforts.
- Thresholds can be experimentally found as values that improve detection.

We will begin with analysis of our data. We will fit distributions to our data, as appropriate, and perform a $\chi^2$ goodness-of-fit test for our proposed distributions. We additionally compared our results to theoretical results and other results found in the literature.

We initially examined the plots of the raw data and various forms looking for patterns in the data that could be used to differentiate persons with wires from person without wires.

Firstly, we computed the differences between V (vertical) and H (horizontal) polarization with wires and vest 1 configuration and with wires and vest 2 configuration. We want to show that the RCS differences follow an exponential distribution, see Table 6.

**Table 6.** Descriptive statistics from Excel on our scaled data captured on the *RCS* of the differences between V (vertical) and H (horizontal) polarization. Column 1 represent with wires and vest 1 configuration and column 2 represents with wires and vest 2 configurations.

| Statistic | Vest1 | Vest2 |
|---|---|---|
| Mean | 6.5749 | 6.4058 |
| Standard error | 0.9962 | 0.5485 |
| Median | 3.4825 | 5.782 |
| Mode | 2.4136 | 7.1107 |
| Standard deviation | 6.37889 | 3.51212 |
| Sample variance | 40.69 | 12.335 |
| Skewness | 1.385 | 0.3901 |
| Minimum | 0.1317 | 0.8848 |
| Maximum | 26.7975 | 14.4848 |
| Count | 41 | 41 |

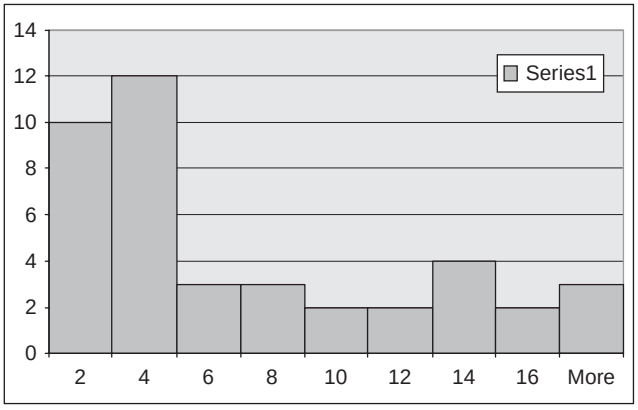


**Figure 18.** Histogram of dataset 1, vest configuration 1.

Firstly, we take the scaled or normalized the data and then display a histogram of the data in vest 1, see Figure 18. We will use the $\chi^2$ goodness-of-fit test to a truncated exponential distribution:

$$H_0: f(x) = \frac{\lambda e^{-\lambda x}}{1 - e^{-\lambda x_0}},\ 0 \le x \le x_0$$

Since our test statistic value is less than our critical value, we conclude that the truncated exponential with empirical mean 0.15209355 is a good fit at an $\alpha$ level of 0.05:

$$\chi^2 = 5.11619$$
$$\chi^2_{.05,4} = 5.11619$$

We perform the same analysis for the data from vest 2, see figure 19.

We tested using a goodness-of-fit test to a truncated exponential distribution:

$$H_0: f(x) = \frac{\lambda e^{-\lambda x}}{1 - e^{-\lambda x_0}},\ 0 \le x \le x_0$$

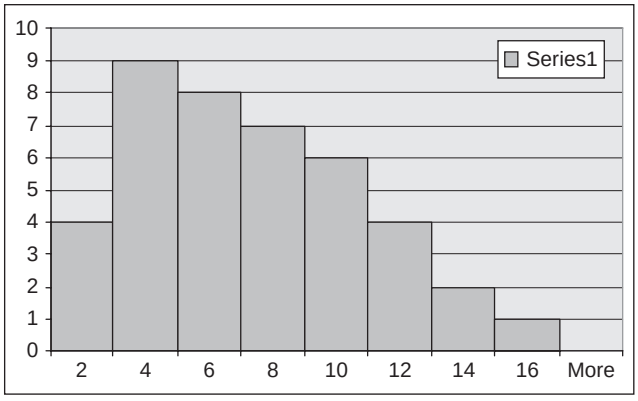


**Figure 19.** Histogram of data set 2, vest configuration 2.

We conclude that the truncated exponential with empirical mean 0.156108622 is a good fit at an $\alpha$ level of 0.05:

$$\chi^2 = 4.6898$$
$$\chi^2_{.05,4} = 9.48$$

Both empirical distributions are essentially exponential distributions and, which is supported by both the literature and others' research.[12] Further, we can look at the mean differences of 6.5749 and 6.405791 with respective standard deviations, 6.37889 and 3.51212, from the sample of size, $n = 41$, and we can evoke the central limit theorem.

This gives us two normal random variables for the mean differences in our two cases: Normal(6.5749, 1.0004) and Normal(6.37889,0.5485), which we will use in a later simulation model.

By capturing the RCS differences, we may compute probabilities, confidence intervals (CIs), or hypothesis tests on the data to measure the statistical evidence of wires on a person.

**Table 7.** Descriptive statistics on persons without wires.

| Human without wires | |
|---|---|
| Mean | 0.965609756 |
| Standard error | 0.107658023 |
| Median | 1.19 |
| Mode | 1.45 |
| Standard deviation | 0.689347694 |
| Sample variance | 0.475200244 |
| Kurtosis | –1.795330031 |
| Skewness | –0.148915314 |
| Range | 1.8 |
| Minimum | 0 |
| Maximum | 1.8 |
| Sum | 39.59 |
| Count | 41 |

Obviously one problem is going to be false positives. We will detect not only wires and metal canister bombs on persons, but also cell phones hung around the neck and jewelry worn on the body.

We tested the information from the human body without wires. We obtained the descriptive statistics in Table 7.

We performed a chi-squared goodness-of-fit test for this data and exponential distribution with a mean of 0.965609756 using the same technique as described earlier. Since 1.249163 < 9.48, we fail to reject that distribution is exponential with mean 0.965609756 and conclude that it is a good fit.

We also analyze if our data supports the theory that the RCS of a human being is 1 $m^2$. We will use a simple hypothesis test:[17]

$$H_0 : \mu = 1$$
$$H_a : \mu \neq 1$$

Using a 0.05 level of significance, we obtain a critical value of $z_{a/2} = 1.95$ The test statistic is –0.3195. Since –0.3195 < 1.96, then we fail to reject the null hypothesis. We confirm that the mean RCS of a human is 1 $m^2$.

We note in Figure 20 that there are similarities in the two curves for the VV and HH polarization similar to the work of Dogaru et al.,[12] explained earlier. We also fail to see large differences in two polarizations.

Plots of our subjects with wire loop and wire loop and triggers are illustrated in Figures 21 and 22. In these figures, we see a wider gap between the polarizations indicating a possible metric, the absolute difference in polarization or the ratio of polarizations.

These plots again clearly show that there is a visual difference between the RCS with VV and HH polarization when wires are on our subjects. Therefore, we will conclude that a possible metric for identifying wires on a person can be accomplished through the difference between the VV and HH RCS measurements. We will discuss the use of this metric later. We used the data from Table 1.

We continued our search for possible metric variables that indicate a difference between a person and a person without wires on their bodies. We next tried polarization ratio; VV/HH was examined as a possible metric for identifying persons with wires. The results from the 10.25 GHz GunnPlexer measurements described above are summarized in Table 8.

The polarization ratio for the cases where the subject has wires on their person is shown to be significantly different from the case without wires, given the level of uncertainty in the measurements. We will use hypothesis tests, comparing the mean ratio, to accomplish this test.

It appears as though the larger the ratio the more likely it is that a subject is wearing wires. Also notice that the ratio for the human without wires was almost 1 $m^2$. Again, this is consistent with the human body having a RCS of 1 $m^2$ regardless of polarity, as seen in Figure 20.

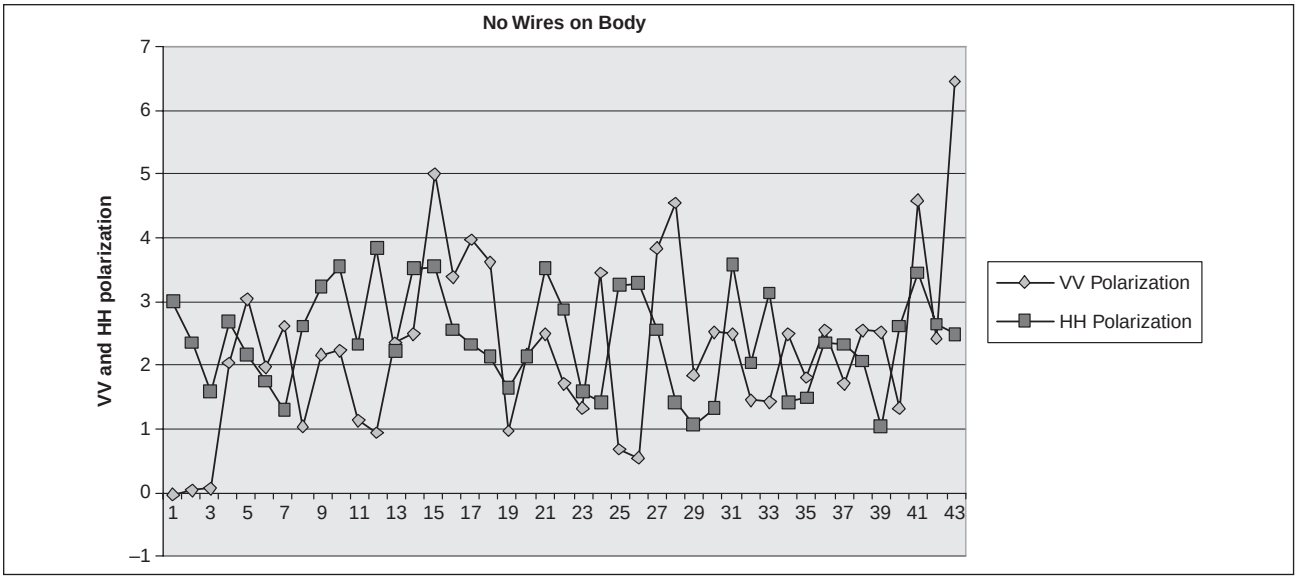


**Figure 20.** Plot of persons (RCS differences) without wires.

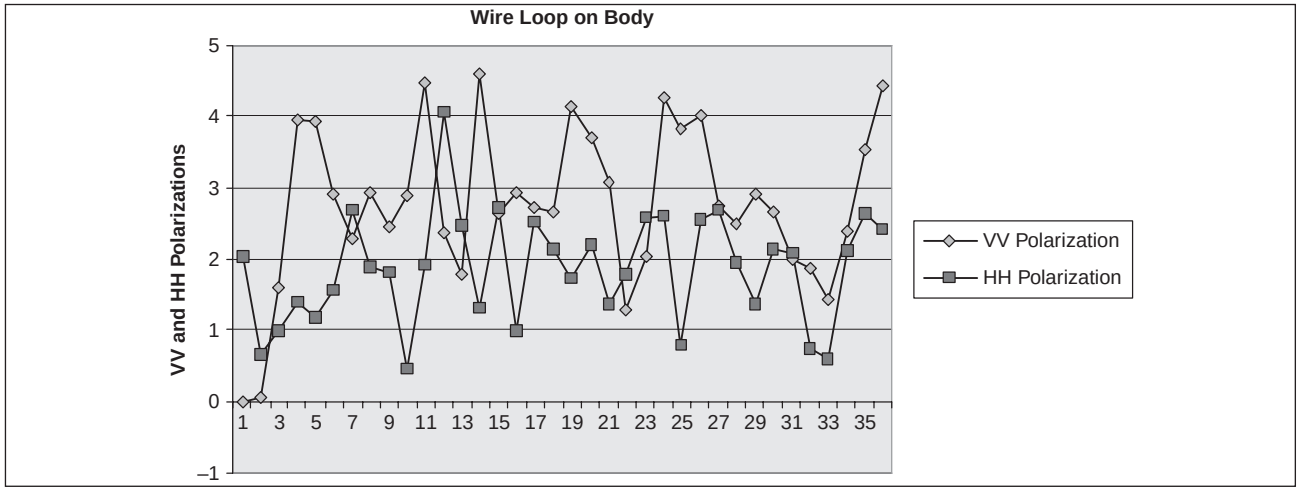


**Figure 21.** Plot of RCS differences for persons with wires in vest configuration 1.

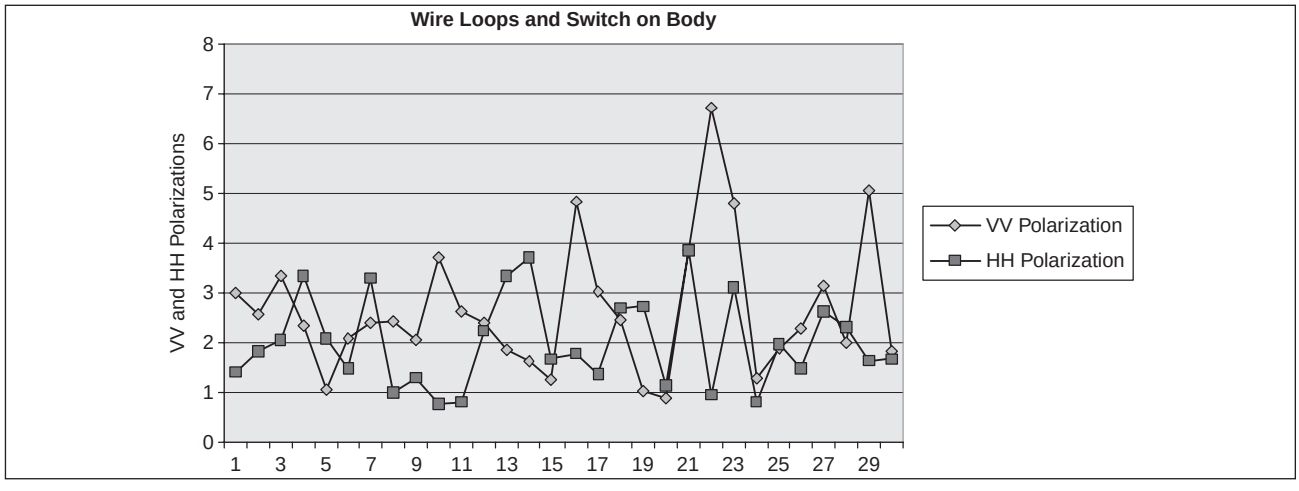


**Figure 22.** Plot of RCS differences for persons with wires in vest configuration 2.

**Table 8.** Measurements from GunnPlexer.

| Experiment | Description | RCS VV | RCS HH | Ratio | SE |
|---|---|---|---|---|---|
| #2 & #3 | No metal | 2.44 | 2.37 | 1.03 | 0.12 |
| #4 & #5 | Loop around waist | 2.78 | 1.80 | 1.52 | 0.15 |
| #7 & # 8 | Loop around waist & wire down sleeve | 2.87 | 2.00 | 1.43 | 0.11 |

The higher or lower ratios (depending upon HH/VV or VV/HH) are shown to be significant indicators of wires on humans, as seen in Figures 21 and 22. We analyzed the hypothesis test as follows for the three cases to insure that we can measure statistical significance in differences of the means.

Case 1:
$H_0 : \mu_1 = \mu_2$
$H_a : \mu_1 \neq u_2$

Case 2:
$H_0 : \mu_1 = \mu_3$
$H_a : \mu_1 \neq u_3$

Case 3:
$H_0 : \mu_2 = \mu_3$
$H_a : \mu_2 \neq u_3$

The rejection region with $\alpha$ =0.05 in each case is reject if $|Z| > 1.96$.

The test statistics are:

Case 1: $|Z| = |1.03–1.520/(0.1425)| = 3.439$
Case 2: $|Z| = |1.03–1.430/(0.1628)| = 2.457$
Case 3: $|Z| = |1.52–1.43/(0.186)| = 0.483$

Since our comparison of Case 1 to Case 2 are statistically significant ($\alpha$=0.05) then our metric, the differences in polarization to identify wires on person, is justified.

Another quick method to get information quickly is via CIs. We provide 95% CIs[17] for the mean ratios in this case:

$$\bar{X} \pm z_{\frac{\alpha}{2}} \frac{s}{\sqrt{n}}$$

Since we are dealing with a large sample and means, we assume the central limit theorem holds and use the normal distribution. We will assume $\alpha$ is 0.05 for this analysis.

We present the results of building a CI for the three ratios:

no metal: the 95% CI is between [0.7948, 1.2652];
wire loops: the 95% CI is between [1.226, 1.814];
wire loop and wire down sleeve: the 95% CI is between 1.2144, 1.6456].

We note that there is an overlap of the 95% CI of all three different experiments. We should be concerned with this overlap, which is where there is the potential for identifying 'false positives'. This region from about 1.2144 to 1.2652 is a region where more analysis is required. In addition, in our modeling this single metric, which might be in doubt, should be used with an additional metric for clarification.

## *4.2 Target Speed and the Pace of Life Metric*

In previous analysis done by Bornstein and Bornstein[4] on 'The Pace of Life', they calculated the average speed a person walks in various cities of the world as a function of the size of the population. There were four Middle Eastern cities in their analysis with average walking speeds of 3.70, 3.27, 4.31, and 4.42 ft/s. It is our further hypothesis that a

**Table 9.** Simulations results from VV-HH differences for 36 runs of 1000 trials each.

| Suicide bombers | Not suicide bombers |
|---|---|
| Mean | 0.560787438 | 0.543975052 |
| Standard error | 0.034917055 | 0.019330647 |
| Median | 0.585714286 | 0.559027778 |
| Mode | 0.5 | 0.5 |
| Standard deviation | 0.20950233 | 0.115983885 |
| Sample variance | 0.043891226 | 0.013452262 |
| Kurtosis | –0.034954882 | 0.757669734 |
| Skewness | 0.265457119 | –0.768842667 |
| Range | 0.833333333 | 0.516908213 |
| Minimum | 0.166666667 | 0.222222222 |
| Maximum | 1 | 0.739130435 |
| Sum | 20.18834776 | 19.58310187 |
| Count | 36 | 36 |

**Table 10.** Simulations results from VV/HH ratio for 36 runs of 1000 trials each.

| Suicide bombers | False positives | |
|---|---|---|
| Mean | 0.834174 | 0.28081 |
| Standard error | 0.020971 | 0.030595 |
| Median | 0.845238 | 0.307692 |
| Mode | 1 | 0 |
| Standard deviation | 0.125823 | 0.183571 |
| Sample variance | 0.015831 | 0.033698 |
| Kurtosis | –1.12174 | –1.05429 |
| Skewness | –0.19122 | –0.19534 |
| Range | 0.4 | 0.6 |
| Minimum | 0.6 | 0 |
| Maximum | 1 | 0.6 |
| Sum | 30.03027 | 10.10915 |
| Count | 36 | 36 |

suicide bomber will not walk at the same speed as everyone else and that their speed can be a further metric to remove the false positives. The Doppler can provide information about the speed of the subject under investigation because of suspected wires. This speed of the subject, if either to slow or to fast as differentiated from the norm in the region, can be used to help support the finding of a target.

For example, the average speed of a Middle Eastern person is normally distributed with a mean of 3.925 and a standard deviation of 0.5394.

We performed a hypothesis test using a level of significance of 0.05 (0.025 in each tail):

$$H_0 : \mu = 3.925$$
$$H_a : \mu \neq 3.925$$

The average speed of the subject is found by the radar to be 4.5 f/s from 36 reads. The test statistic is $z = 6.39$.

The rejection region is to reject the null hypothesis when $Z \geq Z_{\alpha/2}$ and reject it if $Z \geq |1.96|$. We find $6.39 \geq |1.96|$, so we reject the null hypothesis and conclude that the speed of the subject is not consistent with normal speed in the region.

The individual's speed (if the assumption holds) gives us another metric in our detection analysis.

We have various metrics to use in our analysis: RCS differences, RCS ratios, and speed. We looked at a Monte Carlo simulation model of simple, single radar scanning a crowd with a suicide bomber in the crowd. The simulation algorithm employed was easily converted into a simple simulation within Excel.

## *4.3 Simulation Modeling*

The Monte Carlo simulation algorithm[16] we developed to use in our simulation is as follows.

INPUTS: $N$, number of runs, assumed distribution for the number of suicide bombers in a crowd, distributions for probability metric for radar detections, threshold value.
OUTPUTS: the number of positive detections, the number of false detections.

Step 1. Initialize all counters: detections = 0, false alarms=0, suicide bombers =0.
Step 2. For $i = 1,2,\ldots, N$ runs do.
Step 3. Generate a random number from an integer interval $[a,b]$.
Step 4. Obtain an event of a suicide bomber based upon a hypothesized distribution of the number of suicide bombers in a crowd of size $X$. Basically, if a random number $\leq a$ then we have a suicide bomber, otherwise we do not.
Step 5. Generate a random number from the distribution of VV–HH differences, depending on whether the target is a suicide bomber with a vest and wires or not a suicide bomber. These distributions are described previously in this section.
Step 6. Compare the results from step 5 to the threshold value using the following:
target present: $y(t) > Y \rightarrow$ correct detection;
target present: $y(t) < Y \rightarrow$ missed detection;
target not present: $y(t) > Y \rightarrow$ false alarm;
target not present: $y(t) < Y \rightarrow$ no action.
Step 7. Increase counters as necessary;
Step 8. Output descriptive statistics.
END

The purpose of the Monte Carlo simulation models is two-fold. Firstly, we want to make thousands of runs and capture statistics on identifying positive and false targets. Secondly, the simulation allows us to test various simplified scenarios without putting individuals in harm's way.

The threshold of differences was chosen experimentally as 5.08. We ran numerous trials and captured values for the number of suicide bombers, the number of found targets, the number of bombers missed by the simulation detection techniques, and the number of false positives. We repeated the simulation runs of 1000 trials 36 times each.

We found 100% of the suicide bombers only 8.33% of the time using just the absolute differences in polarization. On average we found 56% of the suicide bombers created in the simulation. On average, we found false targets 54.39% of the time. These 54.39% will require an additional metric to exclude these possible subjects. These results are slightly better than random checks (50–50) by guessing, see Table 9.

We repeated the simulation, replacing the metric of differences with the metric using polarization ratio data. Simulation 2 used the ratios in the RCS to generate the detection of the suicide bombers and capture statistics. Step 5 now uses the ratios and their respective distributions.

The threshold of differences was chosen experimentally as 1.35. We ran 1000 trials and captured values for the number of suicide bombers, number of found targets, number of bombers missed by the simulation detection techniques, and number of false positives. We repeated the simulation runs to obtain 36,000 trials. Again, we used Excel to perform the algorithm.

We found 100% of the suicide bombers 22.22% (an increase of 14% over the differences) of the time using just ratios. On average we found 83.42% of the suicide bombers created in the simulation, see Table 10. On average, we found false targets 28.08% of the time.

Through these simulations, we conclude that through using the ratio of RCS VV to HH we obtain better detecting results. We found on average 30% more suicide bombers and had a decrease of 30% in false detections. Again, our initial simulation model does not include the speed of the target as a metric. Including this metric should improve the statistics of detecting the target, as well as further decreasing the false positives.

We went back to our simulation 2 and added in the assumption about walking speed being normally distributed (3.925, 0.54) for a normal person and significantly less for a suicide bomber. We are able to detect 100% of the suicide bombers. The speed metric yielded an increase in false positives due to speed only, but that number is significantly reduced with our RCS ratio metric. However, when coupled with the other metrics for detection and false positives, it did not significantly affect those probabilities in our simulation cases (using the polarization ratios).

## 5. Findings, Conclusions, and Recommendations

We had many findings and conclusions. We highlight several of the more important findings and conclusions below followed by our recommendations.

- Finding: a simple CW Doppler radar can provide valuable experimental data that are very useful in developing the radar technique for detecting persons with wires on their bodies.
  Conclusion: based on our general conclusion that a radar technique for detecting wires on people is feasible, experiments using simple CW Doppler radars, but primarily in the 0.5–3 GHz frequency band, provide a very valuable follow-on step in further exploration and development of radar techniques for detecting persons with wires on their bodies.
- Finding: experimental measurements at 10 GHz of polarization ratios between HH and VV polarizations show a measurable increase when wires are present on a human body.
  Conclusion: the polarization ratio provides a viable metric for distinguishing between human bodies with and without wires using a 10 GHz radar.
- Finding: analysis of the RCS of human bodies with and without wires using numerical electromagnetic techniques indicate that for a RCS metric the best SCR is in the frequency band near 1 GHz. In this frequency band the SCR is about 10 dB over bands of a few 100 MHz.
  Conclusion: future development of radar techniques using a RCS metric will likely prove the most fruitful at frequencies near 1 GHz.
- Finding: analysis of the polarization ratio of radar echoes from the human body with and without wires using numerical electromagnetic techniques indicate that for a polarization ratio metric the best SCR is in the frequency band from about 0.7 to 2.6 GHz. In this frequency band the SCR is above 10 dB over nearly the entire band.
  Conclusion: future development of radar techniques using a polarization ratio metric are likely to prove fruitful at frequencies from about 0.7 to 2.6 GHz.
- Finding: basic radar (a GunnPlexer) was shown to detect wires on a body in various configurations. The better metric was the RCS ratio, VV/HH polarization. Using VV/HH as our metric in the simulation of a single radar scanning a crowd, we were able to correctly detect the target 83.4% of the time. HH polarization ratio, of the RCS yielded very promising results in detection probability. More testing needs to be done in various frequency ranges to find the 'best' frequency range that gives the highest probability of success.
- Finding: using more radars might be better than just one radar.
  Conclusion: If we assume that our probability of successful detection is constant for our radar of choice, then we can use the binomial distribution to test the effectiveness of multiple radars. In detection theory, we use m = *np* and solve for the number *n* to achieve a specific value of m detections. Mathematically, it is shown to be more effective as it increases the detection probability. More testing and experimentation needs to be done to collect and analyze data in this area.
- Finding: speed of motion of the suicide bomber is a good metric and should be used as a variable in the detection scheme. Video might be extremely useful to examine this.
  Conclusion: speed is another good metric used in modeling. This is based upon our assumption that the speed at which a suicide bomber moves in a crowd is substantially different than other crowd members. Testing and video usage experimentation should be accomplished to verify this finding.
- Finding: persons wearing wires will be suicide bombers. We assume no metal jewelry is worn nor will someone wear their cell phone around their neck

Conclusion: this is a simplifying assumption for this phase of the modeling and should be revisited in future modeling efforts.

Based upon our finding we make the following recommendations.

We have shown that radar technology is capable of detecting persons carrying wires on their bodies for the purpose of suicide bombing. We need to make every effort to get the appropriate technology in the hands of those that need it to protect and to save lives.

We had to consider the candidate radar systems: We discuss the system parameters and trade-off considerations that lead to the selection of a baseline design for a prototype that can be field tested. The key considerations are ability to measure the Doppler shift spectrum of echoes, the location of targets, and the ability to measure target cross-section in multiple polarizations. Additional considerations are simplicity, suitability for field use (weight, size, power consumption), and cost. Clearly a system design is beyond the scope of this report.

We investigated and found several radar-based metrics to allow detection of persons wearing wires. From these metrics we built a simulation model that generated a crowd of people and randomly designated some with wires on their bodies. We used our metric and a threshold value, which we determined experimentally, to distinguish the persons with wires form those without wires. The simulations allowed assessment of metrics and determination of their detection and false-alarm rates. We found success through viable metrics for detecting wires on people using radar observations. Our preliminary research shows that suicide bombers can be found prior to the detonation of their bombs and at ranges that are relatively safe.

## Acknowledgements

The authors thank Jerry M Couretas and Vickie Pate for their support. We are also indebted to our reviewers for their excellent suggestions. This work was funded by JON and grant numbers R9QKL and N00244-09-1-0055.

## 6. References

1. Meigs, MC, Gen(R). JIEDDO PowerPoint Update Report to Congress, Director, Joint IED Defeat Organization, 19 November 2007.
2. Kingsley S and Quegan S. *Understanding radar systems*. London: McGraw Hill, 1992.
3. Skolnik MI. *Introduction to radar systems*, 3rd ed. New York: McGraw-Hill, 1992.
4. Bornstein MH and Bornstein H G. The Pace of Life. *Nature* 1976; 259: 557–559.
5. Angell A and Rappaport C. Computational modeling analysis of radar scattering by metallic body-worn explosive devices covered with wrinkled clothing. *IEEE MTT-S Int Microwave Symp Digest* 2007; 6: 1943–1946.
6. Angell A and Rappaport C. Computational modeling analysis of radar scattering by clothing covered arrays of metallic body-worn explosive devices. *Electromagn Waves* 2007; 76: 285–298.
7. Hamid AK. Iterative solution to the TM scattering by two infinitely long lossy dielectric elliptic cylinders. *J Electromagn Waves Appl* 2004; 18: 529–546.
8. Hamid AK. Electromagnetic scattering from a dielectric coated conducting elliptic cylinder loading a semi-elliptic channel in a ground plane. *J Electromagn Waves Appl* 2005; 19: 257–269.
9. Norgren M. A hybrid FDFD-BIE approach to two-dimensional scattering from an inhomogeneous biisotropic cylinder. *Electromagn Waves* 2002; 38: 1–27.
10. Xu X-B and Ao J. A hybrid integral and differential equation method solution of scattering of TM excitation by buried in homogeneous cylinders. *Electromagn Waves* 1997; 15: 165–189.
11. Ciambra F. A spectral-domain solution for the scattering problem of a circular cylinder buried in a dielectric half space. *Electromagn Waves* 2002; 38: 223–252.
12. Dogaru T, Nguyen L and Le C. Computer models of the human body signature for sensing through the wall radar applications. Tech. Rpt. ARL-TR-4290, Army Research Laboratory, 2007.
13. Gabriel C. Compilation of the dielectric properties of body tissue at RF and microwave frequencies. Rpt. AL/EE-TR-1996-0037 USAF School Aerospace Medicine, Brooks AFB, Texas, 1996.
14. Sadiku MNO. *Numerical techniques of electromagnetics*. CRC Press, 1992. 2nd Ed. (2001), Boca Raton, FL., USA.
15. Burke GJ and Poggio AJ. *Numerical Electromagnetics Code (NEC) - Method of Moments*. Springfield, VA: National Technical Information Service (U.S. Department of Commerce), 1981.
16. Fox WP, Giordano F, Horton S and Weir M. *A first course in mathematical modeling*, 4th ed. Belmont, CA: Cengage Publishing, 2009.
17. Devore JL *Probability and statistics for engineering and the sciences*, 5th ed. Pacific Grove, CA: Duxbury, 2000.

## Author Biographies

**Dr William P Fox** is a full professor in the Department of Defense Analysis at the Naval Postgraduate School. He received his BS degree from the United States Military Academy at West Point, New York, his MS at the Naval Postgraduate School, and his PhD at Clemson University. Previously he has taught at the United States Military Academy and Francis Marion University where he was the chair of mathematics for eight years. He has many publications, including books, chapters, journal articles, conference presentations, and workshops. He directs several math modeling contests through the Consortium for Mathematics and Its Applications (COMAP). His interests include applied mathematics, optimization (linear and non-linear),

mathematical modeling, statistical models for medical research, and computer simulations. He is a member of the Military Application Society of the Institute for Operations Research and the Management Sciences (INFORMS).

**Professor John Vesecky** studied Electrical Engineering at Rice University before attending graduate school at Stanford. After academic posts at the University of Leicester UK, Stanford, and Michigan he was selected in 1999 as Founding Chairman of the Electrical Engineering Department in the new Jack Baskin Engineering School at the University of California, Santa Cruz. He has served as Chair or Associate Chair ever since. Recent teaching experience has focused on Capstone Design Courses for undergraduates and the impact of technological innovation on environmental challenges. In the 1990s he served on Vice-President Gore's Environmental Task Force as Chair of the Sensors Panel. His areas of research expertise include radar and radar systems, Earth remote sensing, ocean sensors, and autonomous vehicles. He has a lifelong interest in amateur radio and holds an amateur extra class Federal Communications Commission (FCC) license, AE6TL. He is an Institute of Electrical & Electronics Engineers, Inc. (IEEE) Fellow.

**Adjunct Professor Kenneth** Laws studied Physics at the University of California, finishing with a Doctorate in 2001. Since then he has done research on topics in radar applications to ocean remote sensing, emphasizing the use of high-frequency (HF) (decameter wavelength) radars along the coast line to measure ocean currents. The main thrust of his research has been the analysis of errors in surface current measurements and tracking ships using HF radar. He has also worked with autonomous ocean surface vehicles and renewable energy projects in the coastal environment. His teaching experience includes engineering design classes and bringing the engineering and science aspects of sustainable energy to a wide spectrum of undergraduate students.